THE ROTATION PERIOD OF THE PLANET-HOSTING STAR HD 189733

GREGORY W. HENRY[1] AND JOSHUA N. WINN[2]

[1] Center of Excellence in Information Systems, Tennessee State University, 3500 John A. Merritt Blvd., Box 9501, Nashville, TN 37209, USA
[2] Department of Physics, and Kavli Institute for Astrophysics and Space Research, Massachusetts Institute of Technology, Cambridge, MA 02139, USA

ABSTRACT

We present synoptic optical photometry of HD 189733, the chromospherically active parent star of one of the most intensively studied exoplanets. We have significantly extended the timespan of our previously reported observations and refined the estimate of the stellar rotation period by more than an order of magnitude: $P = 11.953 \pm 0.009$ days. We derive a lower limit on the inclination of the stellar rotation axis of 54° (with 95% confidence), corroborating earlier evidence that the stellar spin axis and planetary orbital axis are well aligned.

Key words: planetary systems – planetary systems: formation – stars: individual (HD 189733) – stars: rotation

Online-only material: machine-readable table

1. INTRODUCTION

Of all the known transiting exoplanets, in many ways the best target for intensive study is HD 189733b, discovered by Bouchy et al. (1995). The star is nearby and bright ($d = 19$ pc, $V = 7.7$); the planet-to-star radius ratio is relatively large ($R_p/R_\star = 0.16$); and the orbital period is relatively short (2.2 days). Thus, the star grants numerous opportunities to observe deep transits with a high signal-to-noise ratio. Investigators have seized these opportunities to measure the stellar and planetary radii (Bakos et al. 2006; Winn et al. 2007; Baines et al. 2007; Pont et al. 2007), the alignment between the stellar rotation and orbital axes (Winn et al. 2006), the planet's infrared spectrum (Deming et al. 2006; Grillmair et al. 2007), the planet's infrared brightness distribution (Knutson et al. 2007), and the planetary atmosphere (Tinetti et al. 2007).

However, one aspect of HD 189733 is not ideal: the star is relatively active, with strong chromospheric emission (Wright et al. 2004) and a spotted photosphere (Winn et al. 2007; Pont et al. 2007). This activity effectively causes an extra noise of ≈ 12 m s^{-1} in Doppler velocities and $\approx 1\%$ in relative photometry with a characteristic timescale equal to the stellar rotation period, which has been estimated by various means to be 11–13 days (Bouchy et al. 2005; Hébrard & Lecavelier des Étangs 2006; Winn et al. 2007). Because the rotation period is much longer than the transit duration (1.8 h), the activity-related noise can often be neglected in a single-transit study, or it can be accounted for with a simple prescription such as fitting a linear function of time to the out-of-transit Doppler velocities or the relative flux. However, a more sophisticated understanding of the stellar variability is important for very high-precision work and for comparing observations of different transits. For example, the discrepant values for $R_p/R_\star$ that have been obtained by different authors might be explained as the result of spot-pattern variability.

Although the photospheric variations can be a nuisance for high-precision work, they do provide at least one benefit, namely the possibility of measuring the stellar rotation period with great accuracy. If the spot pattern is relatively stable over several rotation cycles, then a quasiperiodicity may be detectable in the stellar flux. The rotation period is a fundamental quantity characterizing the star as well as the angular momentum evolution of the planetary system, and the period can also be used to study the alignment between the stellar rotation axis and the orbital axis (Winn et al. 2007).

In this paper we present optical photometry of HD 189733 spanning three observing seasons, from 2005 October to 2007 July. Our goal is to provide a fuller context for some of the specific datasets that were taken during this timespan, and to help in planning future investigations by setting realistic expectations for the typical variability of this star. In the following section, we describe the observations and the data, and provide the entire data set in electronic form. In Section 3, we use the data to determine the stellar rotation period with much greater precision than has previously been possible. (A portion of the data was presented by Winn et al. (2007), but the expanded dataset presented here allows for tremendous improvement.) In Section 4, we use the improved stellar rotation period to update the determination of the inclination angle of the stellar rotation axis with respect to the sky plane. The last section summarizes the results.

2. OBSERVATIONS AND DATA REDUCTION

We acquired 314 good observations of HD 189733 between 2005 October and 2007 July with the T10 0.8 m automated photometric telescope (APT) at Fairborn Observatory in southern Arizona. The APT uses two temperature-stabilized EMI 9124QB photomultiplier tubes to detect photon count rates simultaneously through Strömgren b and y filters. On a given night, the telescope automatically makes observations of each target star and three nearby comparison stars, along with measures of the dark count rate and sky brightness in the vicinity of each star. Designating the comparison stars as A, B, and C, and the target star as D, the observing sequence is DARK, A, B, C, D, A, SKY$_A$, B, SKY$_B$, C, SKY$_C$, D, SKY$_D$, A, B, C, D. In this case, the target star D was HD 189733, and the comparison stars A, B, and C were HD 189410, HD 191260, and HD 189410, respectively (i.e., we chose to make duplicate observations of HD 189410 rather than use a third comparison star). A diaphragm size of 45″ and an integration time of 20 s were used for all integrations.

The observations were reduced to form three independent measures of each of the six differential magnitudes D−A, D−B, D−C, C−A, C−B, and B−A. These were placed on the standard

Table 1
Individual Photometric Observations of HD 189733

Hel. Julian Date (HJD − 2,400,000)	D−A (mag)	D−B (mag)	D−C (mag)	C−A (mag)	C−B (mag)	B−A (mag)
53,652.6447	2.1426	0.4843	2.1406	0.0020	−1.6563	1.6583
53,652.6652	2.1456	0.4858	2.1469	−0.0014	−1.6611	1.6597
53,652.6932	2.1420	0.4833	2.1425	−0.0005	−1.6592	1.6588
53,653.6206	2.1494	0.4920	2.1505	−0.0012	−1.6586	1.6574
53,653.6416	2.1486	0.4915	2.1514	−0.0027	−1.6598	1.6570

Note. Differential magnitudes were measured in the Strömgren $(b + y)/2$ passband.
(This table is available in its entirety in a machine-readable form in the online journal. A portion is shown here for guidance regarding its form and content)

Strömgren system with yearly mean transformation coefficients. These differential magnitudes were corrected for dead time and differential extinction. To increase the signal-to-noise ratio, the data from the b and y passbands were averaged to create "$(b + y)/2$" magnitudes. After passing quality control tests, the three independent measures of each differential magnitude were combined, giving one mean data point per complete sequence for each of the six differential magnitudes. The standard deviations of a single observation about the means of the 314 D−A, D−B, D−C, C−A, C−B, and B−A differentials are 0.0064, 0.0064, 0.0064, 0.0014, 0.0019, and 0.0018, respectively. Because C and A represent the same star, the C−A standard deviation of 0.0014 mag is a good estimate of the limiting uncertainty in each measurement. The C−B and B−A standard deviations of 0.0019 and 0.0018 mag show that the two comparison stars (A and B) are intrinsically constant to 0.001 mag or better. The much larger standard deviations (0.0064 mag) of the D−A, D−B, and D−C data indicate that HD 189733 is significantly variable. For additional information on the telescopes, photometers, observing procedures, data reduction techniques, and photometric precision, see Henry (1999) or Eaton et al. (2003).

The individual $(b + y)/2$ observations for all six combinations of differential magnitudes are given in Table 1. The time variation of the D−A observations is evident in the top panel of Figure 1. The time series can be divided into four segments of nearly nightly coverage interrupted by long gaps. The first segment is the latter half of the 2005 observing season. The second and third segments are from the 2006 observing season, which is interrupted by the summer shutdown of the APTs during Arizona's rainy season. The fourth segment is from the first half of the 2007 observing season up until the 2007 summer shutdown.

It is clear from Figure 1 that HD 189733 was variable throughout our entire photometric campaign. As noted above, the standard deviation of the complete D−A data set is 0.0064 mag. The standard deviations of the four contiguous time ranges shown in the lower four panels of Figure 1 are (from top to bottom) 0.0058, 0.0044, 0.0083, and 0.0053 mag. From the beginning until approximately JD 2,453,880 (late in May of 2006 and marked with an arrow in Figure 1), the variability was rather erratic. However, from that time forward, the star has exhibited coherent brightness variability until the end of our observations.

3. RESULTS

Chromospherically active stars are often observed to exhibit erratic and occasionally quasiperiodic photometric variability
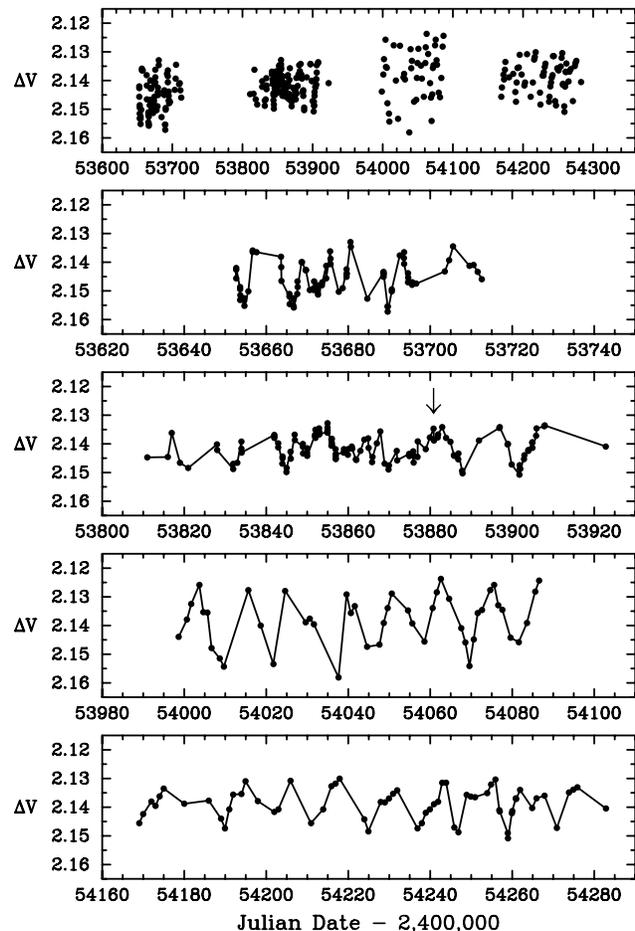

Figure 1. Photometric variability of HD 189733, as observed with the T10 0.8 m APT in the $(b + y)/2$ passband. The magnitude difference between HD 189733 and the comparison star HD 189410 is plotted. The top panel shows the entire data set, while the other panels focus on each of the four segments of near-nightly observations.

(see, e.g., Vaughan et al. 1981; Henry et al. 1995; Lockwood et al. 2007). The quasiperiodic component of the variability is interpreted as the result of photospheric spots and plages that are carried into and out of view as the star rotates (Wilson 1978). The coherence of the star's photometric variation is limited by time variations of the spot pattern on the rotational timescale, as well as emission variations on shorter timescales. Adopting the same interpretation for HD 189733, the spots cover ∼1%–2% of the stellar surface at any moment. Their distribution is apparently complex but was reasonably stable between 2006 May and 2007 July, the time period during which coherent variability was observed (see Figure 1).

This allows us to determine the rotation period of HD 189733 with greater precision than previous estimates. The top panel of Figure 2 shows the frequency power spectrum of the D−A data from JD 2,453,880 onward, computed with the method of Vaníček (1971). This period-finding technique uses the method of least-squares to fit the data with sine curves over a range of trial periods and measures the resulting reduction in the variance of the data. There is a strong peak corresponding to a period of 11.952 days with an estimated uncertainty of 0.016 days. Similar analyses of the D−B and D−C data (the differential magnitudes derived from different comparison
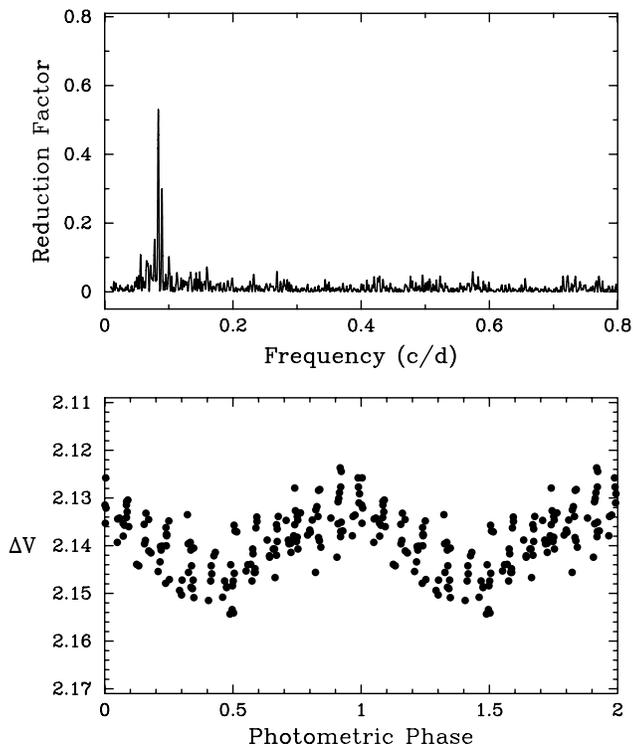
Figure 2. Top: frequency power spectrum of the D−A data, computed with the method of Vaníček (1971). Bottom: phase-folded light curve using the period $P = 11.953$ days.

observations) gave 11.952±0.017 days and 11.955±0.016 days, respectively. These three estimates are all in good agreement. The mean and standard deviation of the mean of these three period determinations give $P = 11.9527 \pm 0.0010$ days, but this precision is probably too optimistic since the three period determinations are not completely independent. Therefore, as our best estimate of the rotation period, we adopt the weighted mean of the three determinations and its formal uncertainty: $P = 11.953 \pm 0.009$ days. The phase-folded light curve is shown in the bottom panel of Figure 2. The quasi-sinusoidal pattern is typical of spot-induced variability with modest cycle-to-cycle spot variations (Henry et al. 1995).

How does this compare to previous estimates of the rotation period? Bouchy et al. (2005) estimated $P \sim 11$ days (but did not venture an uncertainty), based on the combination of the estimated stellar radius, the measurement of the stellar projected rotation velocity $v \sin i$, and the assumption $\sin i = 1$. Hébrard & Lecavelier des Étangs (2006) analyzed the *Hipparcos* photometry for this star and found candidate periods at 13.3, 11.8, 8.8, and 4.6 days. They identified the 11.8-day period as the likely rotation period but did not quantify the uncertainty, as their main concern was identifying planetary transits and refining the estimate of the *orbital* period. A portion of our data were published previously (Winn et al. 2007), yielding the estimate $P = 13.4 \pm 0.4$ days, but that estimate was based on the observation of only 2.5 cycles over approximately 40 days.[3] This is why we cautioned that continued monitoring was needed to check on the period estimate. In contrast, during the

---

[3] In Figure 1 of Winn et al. 2007, the portion that was previously analyzed ranged from the arrow in the central panel to the right-hand edge of the central panel.

full campaign presented in this paper, we observed 18 complete cycles over approximately 400 days.

4. SPIN–ORBIT ALIGNMENT

As alluded to earlier, the measured rotation period can be used to estimate the inclination of the stellar rotation axis with respect to the sky plane. Since the planetary orbit is nearly edge-on, it is natural to suppose the stellar equator is also viewed nearly edge-on, and it is interesting to test this hypothesis. Even if planet formation usually results in the alignment of planetary orbital axes and stellar rotation axis—an assumption that itself is worth checking—some of the planetary "migration" mechanisms that have been proposed to explain close-in giant planets such as HD 189733 could produce large misalignments. In particular, a broad distribution of spin–orbit angles is predicted by theories involving planet–planet scattering (Chatterjee et al. 2007) and Kozai cycles with tidal friction (Fabrycky & Tremaine 2007).

There are at least two observable aspects of spin–orbit alignment. The first aspect is the Rossiter–McLaughlin effect, a spectroscopic distortion that occurs during transits. Observations of this "spectroscopic transit" can be used to estimate the angle λ between the *sky projections* of the stellar rotation axis and the orbital axis (Ohta et al. 2005; Gaudi & Winn 2007). For this system, λ has been measured to be $-1.4° \pm 1.1°$ (Winn et al. 2006).[4] The second aspect is the inclination i of the stellar rotation axis with respect to the sky plane, which can be written in terms of measurable quantities as follows:

$$\sin i = v \sin i \left(\frac{P}{2\pi R_\star} \right). \tag{1}$$

This calculation was done by Winn et al. (2007) using the data available at that time. We update the result using the new value $P = 11.953 \pm 0.009$ days as well as the more precise value $R_\star = 0.755 \pm 0.011 R_\odot$ that has become available through space-based photometry (Pont et al. 2007). The most precise measurement of $v \sin i$ remains unchanged, 2.97 ± 0.22 km s^{-1} (Winn et al. 2006). Assuming Gaussian errors in all these quantities, the result is $\sin i = 0.93 \pm 0.07$.

We estimated the *a posteriori* probability distribution $p(i)$ as follows. For each trial value of i from 0° to 90°, we computed

$$\chi^2 = \left(\frac{\sin i - 0.93}{0.07} \right)^2 \tag{2}$$

and assumed $p(\sin i) \propto \exp(-\chi^2/2)$, leading to $p(i) \propto \exp(-\chi^2/2) \cos i \sin i$. The $\cos i$ factor comes from the transformation of variables from $\sin i$ to i, and the $\sin i$ factor comes from the *a priori* assumption that all orientations are equally likely. The resulting probability distribution and the corresponding cumulative distribution are shown in Figure 3. Although the most probable value of i is formally 65°, we prefer to interpret the result as a lower limit: $i > 54°$ with 95% confidence. This is because $\sin i$ was measured to be consistent with unity within 1σ. Although the probability density vanishes at $i = 90°$, this would

---

[4] Incidentally, the observation that the rotation period is much longer than the orbital period of 2.2 days implies that the two periods have not been tidally synchronized. Since the expected timescale for reorientation of the star is of the same order of magnitude as the timescale for synchronization, this finding supports the interpretation of the observed spin–orbit alignment as primordial, rather than the outcome of tidal effects. For further discussion, see Fabrycky et al. (2007).
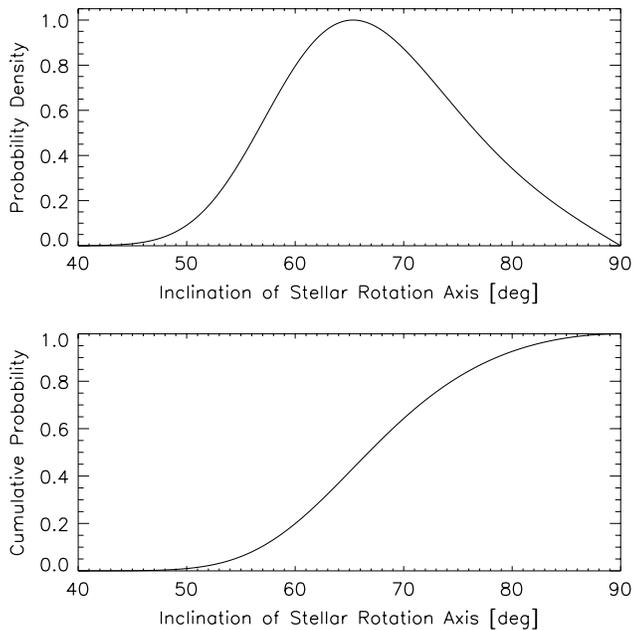
Figure 3. Top: the *a posteriori* probability distribution for i, the inclination of the stellar rotation axis with respect to the sky plane. Bottom: the corresponding cumulative probability distribution. The 95% lower limit on i is $54°$.

be true for *any* measurement of $\sin i$ (even, say, 1.000 ± 0.001) because of the $\cos i$ factor in $p(i)$.

This lower bound is hardly changed at all from the previous result of Winn et al. (2007), and is indeed slightly *less* stringent. The limiting factor is the uncertainty in $v \sin i$, and it is not obvious how further improvement can be made, since the uncertainty is dominated by calibration error rather than random error.

5. SUMMARY

We have presented optical photometry spanning three observing seasons for HD 189733, one of the very brightest stars that has a known transiting planet. During the latter half of our campaign, we detected periodic photometric variations that allowed us to refine the estimated stellar rotation period by more than an order of magnitude. Our photometric data will allow the numerous investigators who carried out intensive transit observations between 2005 and 2007 to assess any spot-induced effects on their data and will help to set realistic expectations for future programs. We confirm the previously published result that the stellar rotation axis is not strongly misaligned with the orbital axis. Given that the intense interest in this object does not seem to be subsiding, we plan to continue the APT observations over the next few seasons.

REFERENCES

Baines, E. K., van Belle, G. T., ten Brummelaar, T. A., McAlister, H. A., Swain, M., Turner, N. H., Sturmann, L., & Sturmann, J. 2007, ApJ, 661, L195
Bakos, G. Á., et al. 2006, ApJ, 650, 1160
Bouchy, F., et al. 2005, A&A, 444, L15
Chatterjee, S., Ford, E. B., & Rasio, F. A. 2007, arXiv:0703166
Deming, D., Harrington, J., Seager, S., & Richardson, L. J. 2006, ApJ, 644, 560
Eaton, J. A., Henry, G. W., & Fekel, F. C. 2003, in The future of Small Telescopes in the New Millennium II. The Telescopes We Use, ed. T. Oswalt (Dordrecht: Kluwer), 189
Fabrycky, D., & Tremaine, S. 2007, arXiv:0705.4285
Fabrycky, D. C., Johnson, E. T., & Goodman, J. 2007, arXiv:0703418
Gaudi, B. S., & Winn, J. N. 2007, ApJ, 655, 550
Grillmair, C. J., Charbonneau, D., Burrows, A., Armus, L., Stauffer, J., Meadows, V., Van Cleve, J., & Levine, D. 2007, ApJ, 658, L115
Hébrard, G., & Lecavelier des Étangs, A. 2006, A&A, 445, 341
Henry, G. W. 1999, PASP, 111, 845
Henry, G. W., Fekel, F. C., & Hall, D. S. 1995, AJ, 110, 2926
Knutson, H. A., et al. 2007, Nature, 447, 183
Lockwood, G. W., Skiff, B. A., Henry, G. W., Henry, S., Radick, R. R., Baliunas, S. L., Donahue, R. A., & Soon, W. 2007, ApJS, 171, 260
Ohta, Y., Taruya, A., & Suto, Y. 2005, ApJ, 622, 1118
Pont, F., et al. 2007, arXiv:0707.1940
Tinetti, G., et al. 2007, arXiv:0707.3064
Vaníček, P. 1971, Ap&SS, 12, 10
Vaughan, A. H., Preston, G. W., Baliunas, S. L., Hartmann, L. W., Noyes, R. W., Middelkoop, F., & Mihalas, D. 1981, ApJ, 250, 276
Wilson, O. C. 1978, ApJ, 226, 379
Winn, J. N., et al. 2006, ApJ, 653, L69
Winn, J. N., et al. 2007, AJ, 133, 1828
Wright, J. T., Marcy, G. W., Butler, R. P., & Vogt, S. S. 2004, ApJS, 152, 261